



ORIGINAL ARTICLE

# How do children with autism spectrum disorder form gist memory during sleep? A study of slow oscillation–spindle coupling

Eva-Maria Kurz<sup>1,2,\*</sup>, Annette Conzelmann<sup>1,3</sup>, Gottfried Maria Barth<sup>1</sup>, Tobias J. Renner<sup>1</sup>, Katharina Zinke<sup>4,†,⊕</sup> and Jan Born<sup>4,5,6,†</sup>

<sup>1</sup>Department of Child and Adolescent Psychiatry, Psychosomatics and Psychotherapy, University Hospital of Psychiatry and Psychotherapy, Tübingen, Germany <sup>2</sup>Graduate Training Centre of Neuroscience, International Max Planck Research School, University of Tübingen, Tübingen, Germany <sup>3</sup>PFH – Private University of Applied Sciences, Department of Psychology (Clinical Psychology II), Göttingen, Germany <sup>4</sup>Institute of Medical Psychology and Behavioral Neurobiology, University of Tübingen, Tübingen, Germany <sup>5</sup>Werner Reichardt Centre for Integrative Neuroscience, University of Tübingen, Tübingen, Germany <sup>6</sup>German Center for Diabetes Research (DZD), Institute for Diabetes Research & Metabolic Diseases of the Helmholtz Center Munich at the University Tübingen (IDM), Tübingen, Germany

<sup>†</sup>These authors contributed equally to this work.

\*Corresponding author. Eva-Maria Kurz, Department of Child and Adolescent Psychiatry, Psychosomatics and Psychotherapy, University Hospital of Psychiatry and Psychotherapy, Tübingen, Germany. Email: [eva-maria.kurz@med.uni-tuebingen.de](mailto:eva-maria.kurz@med.uni-tuebingen.de).

## Abstract

Sleep is assumed to support memory through an active systems consolidation process that does not only strengthen newly encoded representations but also facilitates the formation of more abstract gist memories. Studies in humans and rodents indicate a key role of the precise temporal coupling of sleep slow oscillations (SO) and spindles in this process. The present study aimed at bolstering these findings in typically developing (TD) children, and at dissecting particularities in SO-spindle coupling underlying signs of enhanced gist memory formation during sleep found in a foregoing study in children with autism spectrum disorder (ASD) without intellectual impairment. Sleep data from 19 boys with ASD and 20 TD boys (9–12 years) were analyzed. Children performed a picture-recognition task and the Deese–Roediger–McDermott (DRM) task before nocturnal sleep (encoding) and in the next morning (retrieval). Sleep-dependent benefits for visual-recognition memory were comparable between groups but were greater for gist abstraction (recall of DRM critical lure words) in ASD than TD children. Both groups showed a closely comparable SO-spindle coupling, with fast spindle activity nesting in SO-upstates, suggesting that a key mechanism of memory processing during sleep is fully functioning already at childhood. Picture-recognition at retrieval after sleep was positively correlated to frontocortical SO-fast-spindle coupling in TD children, and less in ASD children. Critical lure recall did not correlate with SO-spindle coupling in TD children but showed a negative correlation ( $r = -.64, p = .003$ ) with parietal SO-fast-spindle coupling in ASD children, suggesting other mechanisms specifically conveying gist abstraction, that may even compete with SO-spindle coupling.

## Statement of Significance

This is the first study to compare the coupling of sleep slow oscillations (SO) with spindles and its relationship to memory formation between healthy children and children with autism spectrum disorder (ASD) without intellectual impairment. Both groups show a comparable coupling of fast spindle activity to the SO-upstate. In TD children, this SO-fast spindle coupling was correlated with retention of visual recognition memory. By contrast, the sleep-associated formation of gist memory, which was enhanced in ASD children, did not correlate with SO-spindle coupling in the healthy children and correlated even negatively with SO-spindle coupling in children with ASD, suggesting additional mechanisms specifically mediating gist abstraction during sleep.

**Key words:** sleep; memory; consolidation; spindles; slow oscillations; children; autism

Submitted: 21 July, 2020; Revised: 28 October, 2020

© Sleep Research Society 2020. Published by Oxford University Press on behalf of the Sleep Research Society.

This is an Open Access article distributed under the terms of the Creative Commons Attribution-NonCommercial License (<http://creativecommons.org/licenses/by-nc/4.0/>), which permits non-commercial re-use, distribution, and reproduction in any medium, provided the original work is properly cited. For commercial re-use, please contact [journals.permissions@oup.com](mailto:journals.permissions@oup.com)

## Introduction

Sleep supports the consolidation of newly acquired memories [1, 2]. Memory processing during sleep has been conceptualized as an “active systems consolidation” process, in which representations that are encoded in hippocampal and neocortical networks are reactivated during sleep, which helps to gradually transform the representations such that they eventually become less dependent or even independent of the hippocampus. The transformation process implicates qualitative changes in the representation, leading to the abstraction of more schema-like memories that only carry the gist of the original experience but lack detailed information about this experience [3, 4]. Memories for gist are thought to become represented in neocortical structures such as the medial prefrontal cortex [5].

Sleep oscillations that have been proposed to drive the consolidation process are the neocortical slow oscillation (0.1–1.5 Hz, slow oscillation [SO]) with a nested fast spindle (12–15 Hz) during the depolarizing SO-upstate, with the spindle oscillations nesting ripples and memory reactivations in hippocampal networks (80–140 Hz) [2, 3]. In mice, the precisely timed triple-coupling of SOs, spindles, and ripples benefited the consolidation of hippocampus-dependent memory [6], and studies in adult humans confirmed the coupling of fast spindles to the SO-upstate to be particularly important for memory consolidation [7–9]. Forgetting in older adults was associated with a “mis-timed” SO-fast spindle coupling [7]. In patients with mild cognitive impairment, slowly oscillating transcranial direct current stimulation (tDCS) during a nap enhanced SO–spindle synchronization compared to sham, and stronger synchronization during stimulation was associated with improved overnight memory retention [10]. Note, these findings in humans refer to the classical fast spindles (12–15 Hz). By contrast, the relationship to memory of slow spindles (9–12 Hz) that are more prominent over the frontal cortex and typically occur at the up-to-down transition of the SO, remains obscure [8, 11–13].

Similar to adults, an increase of fast spindle power during the SO upstate has also been demonstrated in adolescents and children [14, 15]. Precision of SO–spindle coupling increased with age, and this change in coupling precision at frontal recording sites was positively correlated with the change in sleep-dependent memory performance from childhood to adolescents (although, on average, sleep-dependent change in memory did not differ between childhood and adolescence) [14]. Besides, separate associations of overnight memory retention with either sign of enhanced spindle or SO activity have been repeatedly observed in children [16–19].

Autism spectrum disorder (ASD) is a neurodevelopmental disorder that can show both sleep disturbances [20] and specific memory deficits [21, 22]. Due to the heterogeneity of the disorder itself and methodological differences among studies, no consistent pattern regarding microstructural sleep alterations in ASD has been identified so far [23]. Findings range from reduced spindle power [24, 25] or spindle density [26, 27] to increased delta [25] and theta power [28] in ASD children. Some studies did not find any remarkable differences for the spindle and SO characteristics and power between children with ASD and typically developing (TD) children [29, 30]. Correspondingly, sleep-dependent declarative memory consolidation was found to be intact in children with ASD [24, 29, 30], although the ASD children in some of these studies showed an overall worse accuracy

of memory performance in comparison with TD children [29, 30]. In the Fletcher et al. [24] study, the overnight gain in reaction times (one of the indicators of memory for animals) was associated with increased spindle density and sigma power in ASD children. Interestingly, in a previous study of ours, employing a Deese–Roediger–McDermott (DRM) false memory paradigm [31, 32], which was based on free recall, we found signs of gist memory abstraction during sleep to be even enhanced in ASD children [29]. This enhancement in gist abstraction was not a consequence of the generally lower recall performance in the ASD children because the recall of veridical memories was positively (rather than negatively) correlated with gist memory recall in the ASD children.

Considering growing evidence identifying SO–spindle coupling as an essential mechanism supporting systems memory consolidation during sleep, the present study aimed at a fine-grained analysis of SO–spindle coupling and how it relates to the overnight retention of visual recognition memories and abstraction of gist memory, using a data set from a previous study of ASD and TD children [29]. Our focus on SO and spindles was owed to the fact that gist abstraction during sleep—although itself representing an implicit memory process—is thought to arise from the formation of explicit declarative (i.e. hippocampus-dependent) memory [3, 4, 33]. Because the sleep macro- and microarchitecture was entirely normal in the ASD children, we expected that the analysis of SO–spindle coupling would allow identifying a discrete mechanism underlying the enhanced overnight abstraction of gist memory observed in these children. Based on the presently available literature, we expected that enhanced phase-coupling of fast (but not slow) spindles to the SO cycle, as a more precise indicator of systems consolidation of memory during sleep, would be positively correlated to both visual recognition performance (in all children) as well as to the recall of critical lures after sleep. The latter association was expected to be particularly pronounced in the ASD children who previously showed enhanced gist abstraction after sleep compared to wake.

## Methods

### Participants

Analyses were performed on data from a previous study of sleep in 19 boys with ASD and 20 TD boys (age 9–12 years) [29]. None of the participating children had an IQ below 85 as assessed by the Culture Fair Intelligence test (CFT-20-R [34]). All TD children and 16 children with ASD attended mainstream schools. Three children with ASD attended specialized schools ( $n = 1$  focus on language training,  $n = 1$  focus on social and emotional development,  $n = 1$  focus on physical and motor development). Children with ASD met the ASD diagnosis according to the DSM-5 criteria as assessed with the Autism Diagnostic Observation Schedule [35] and/or the Autism Diagnostic Interview-Revised [36], which were conducted by an experienced child and adolescent psychiatrist (GMB). TD children were excluded in case of any clinically relevant behavioral problems or the presence of a psychiatric disorder as assessed through clinical questionnaires (behavioral problems – CBCL/4–18 [37]; social responsiveness – SRS [38]; ADHD related symptoms – DISYPS-II [39]; depressive symptoms – DIKJ [40]; sleep problems – SDSC [41]) and a diagnostic interview (Kiddie-SADS-Present and Lifetime [42]). The

semistructured interview, which was used to confirm comorbid diagnoses in ASD patients and to exclude any psychiatric disorders in the TD children, was conducted by the experimenters (two physicians in training and one psychologist). As previously reported, ASD children exhibited significantly more behavioral and sleep problems than TD children as assessed by the questionnaires (all  $p < .001$ ). None of these measures correlated significantly with our memory measures of interest across groups (all  $r > -.29$ , all  $p > .07$ ). Moreover, including these measures or medication intake as covariates in our target analyses did not substantially alter any of the group differences and correlations reported here.

The study was approved by the ethics committee of the Faculty of Medicine of the University of Tübingen and all participants and their parents gave written informed consent. All children with ASD were recruited via the outpatient clinic for ASD and an ASD specialized training program at the Department of Child and Adolescent Psychiatry, University Hospital of Tübingen. Thus, an ASD diagnosis was existing prior to inclusion in the study. TD children were recruited via the university's mailing system and a database.

## Procedures

All children participated in a pre-experimental session which was used for diagnostics and assessment of intelligence and clinical questionnaires. The experimental sessions, consisting of a Sleep and a Wake condition, were carried out at the participant's home with the order of conditions balanced across participants. Both conditions comprised an encoding session and a retrieval session with the retention interval between the sessions covering an ~11-h interval of daytime wakefulness (Wake) or night-time sleep (Sleep) with sleep recorded polysomnographically. Both conditions comprised two learning tasks, a picture recognition task [43, 44] and the DRM [31, 32] task (see [29] for details). In brief, in the encoding session, the children were asked on the picture recognition task to rate 72 neutral and 72 negative pictures regarding arousal and valence, and on the DRM task listened to eight wordlists each containing 12 highly semantically related words, with each list lacking the word with the strongest common associate (the "critical lure"). On both tasks, the participants were instructed to try to remember as many of the stimuli as possible. In the retrieval session, recognition of the pictures was assessed by presenting the old pictures of the encoding session randomly intermixed with 36 new negative and 36 new neutral pictures. For each picture, the participant had to indicate whether the picture was "old" or "new." The children were instructed to respond spontaneously, but there were no instructions to speed (i.e. to respond as fast as possible) on both tasks. Accordingly, we did not analyze reaction times. On the DRM task, memory for the wordlists was assessed by a free recall. The beginning of the encoding sessions was based on the children's habitual bed and rising times, with the encoding session in the Wake condition starting 1 h after the children woke up, and in the Sleep condition starting 3 h before their habitual bedtime.

For the current question of interest, only memory measures obtained from the Sleep condition were analyzed. Memory on the picture recognition task was assessed by the number of old pictures correctly recognized as old minus new pictures

incorrectly recognized as old neutral and negative pictures, respectively (= adjusted recognition). On the DRM task, veridical memory was determined by the number of correctly recalled words. Gist memory was assessed by the number of (falsely) recalled critical lures (that represented the strongest common associate of a list but had not been presented at encoding) and further analyzed as the proportion of the total recall (of veridical plus critical lure words).

## Sleep recordings

In the Sleep condition, sleep was continuously recorded using a portable recording system (SOMNOscreen plus Neuro+, SOMNOmedics GmbH). Polysomnography recordings (sampling rate 256 Hz) included electroencephalography from F3, F4, C3, Cz, C4, P3, and P4 (referenced to linked mastoids, FPz as ground), two electromyogram electrodes and two electrooculogram electrodes. Preprocessing included a 50 Hz Notch filter, a 0.3–35 Hz bandpass filter for the EEG and EOG, and a 10–100 Hz filter for the EMG. Offline sleep scoring was done for 30-s epochs according to standard criteria [45] to determine total sleep time (TST), wake after sleep onset (WASO), time spent in non-rapid eye movement (non-REM) stages 1 and 2 and slow-wave sleep (SWS, stage 3 plus stage 4), as well as time spent in REM sleep. Scoring was done by experienced staff (EMK, KaZ, study nurse), with an inter-rater agreement >85%. In the case of ambiguous epochs, the scorers discussed the critical epochs and decided together for a sleep stage.

## Spindle detection

Sleep spindle detection during artefact-free non-REM sleep (stages 2–4) was done using the free software SpiSOP (<https://www.spisop.org>; RRID: SCR\_015673). Briefly, the data was first bandpass filtered (two-pass, FIR filter) in the frequency band of interest, i.e. 9–12 Hz for slow spindles and 12–15 Hz for fast spindles. For each participant, the root mean square (RMS) signal was determined for 0.2-s windows, which was then smoothed by a moving average (0.2-s window). A spindle was detected whenever this smoothed moving RMS window exceeded an individual threshold (1.5 SDs of the filtered signal in the respective channel) for 0.5–3 s. The detection algorithm has been used in several previous studies (e.g. [46, 47]). Its validity is routinely checked in each experiment by experienced staff, by visually inspecting the detected spindles. For each participant and separately for slow and fast spindles, we determined the average frontal (F3/F4), central (C3/Cz/C4), and parietal (P3/P4) spindle density (spindle number per 30-s), duration (ms), and amplitude (trough to peak potential,  $\mu$ V).

## Slow oscillation detection

Detection of SOs during artefact-free non-REM sleep epochs was also done using SpiSOP. The EEG signal was high (0.3 Hz) and low pass (4 Hz) filtered. Time intervals with positive to negative zero crossings in the range of 0.5–1.25 Hz (corresponding to 0.8–2 s) were marked as potential SOs. For each channel, the mean potential from the down zero-crossings to the maximum trough (downstate peak), as well as the mean amplitude from maximum trough to peak potential were calculated for all putative SOs. Only those putative SOs were considered as SO whose downstate peak

potential was lower than the mean downstate peak potential multiplied by 1.25 and whose amplitude was larger than the mean amplitude of all putative SOs multiplied by 1.25. For each participant, we determined the average frontal, central and parietal SO density (number of SOs per 30-s epoch), SO duration (ms), and amplitude (maximum trough to peak potential,  $\mu\text{V}$ ).

### Phase-coupling of slow oscillation and spindles

Phase-coupling analyses were performed on all spindles and SOs detected during non-REM sleep epochs. As there is, to the best of our knowledge, no firm evidence for qualitative differences in SO–spindle complexes occurring during stage 2 sleep (here termed also K-complexes) and during SWS (e.g. [48]), we combined data from both sleep stages. In a first step, *peri-event time histograms* were calculated separately for the occurrence of fast and slow spindles, referenced to the maximum trough (downstate peak) of a detected SO event. For this, SO–spindle co-occurrence was first determined by the number of spindle centers (i.e. the maximum spindle trough) occurring within a  $\pm 1.2$ -s window around the downstate peak of a SO, expressed as the ratio of all detected SO events in an individual channel. Ratios were then averaged (for each participant) across frontal, central and parietal channels. Peri-event time histograms of spindle occurrence were calculated for  $\pm 1.2$ -s windows around the SO downstate peak, for 100-ms bins. The number of spindle events per bin was expressed as a percentage with the total number of spindles co-occurring with a SO in each channel set to 100%. Percentages of spindle center occurrence were further averaged across frontal, central, and parietal channels within each individual.

In a second step, we calculated time–frequency representations (TFRs) using the open-source toolbox FieldTrip [49]. For this, time–frequency analyses were applied using Morlet wavelets (cycles increasing linearly from 4 to 12), to a  $\pm 3$ -s window around (the downstate peak of) a SO event; the analysis was performed between 5 and 20 Hz, with steps of 0.5 Hz and 3.9 ms. TFRs were first averaged for all SO events in a channel and, then, over frontal, central, and parietal channels within each participant. Power in each recording site was then normalized to the average power in the  $\pm 1.5$ -s around the SO downstate peak which was set to 100%.

In a third step, *cross-frequency coupling* was assessed based on the synchronization index (SI) [50], to evaluate whether power fluctuations within the spindle frequency band are modulated by the activity in the SO frequency band [10, 13]. For this, the EEG signal within a  $\pm 3$ -s window around (the negative peak of) a SO event was first bandpass filtered in the SO frequency band (0.5–1.25 Hz, two-pass FIR filter, filter order: three cycles of the low frequency cut off). For the spindle frequency bands, the baseline normalized power was averaged across the respective TFR frequency bins for each SO event. This was done separately for the slow (9–12 Hz) and fast (12–15 Hz) spindle frequency bands. Then, the phase values of the SO low-frequency time series and of the high-frequency spindle power time series were extracted using the Hilbert transform. To avoid edge effects, the two time series were cut to  $\pm 1$ -s around the SO negative peak, and the SI was calculated according to the formula:

$$SI = \frac{1}{n} \times \sum_{t=1}^n e^{i[\phi_{lt} - \phi_{ut}]}$$

where  $n$  refers to the number of time points,  $\phi_{lt}$  to the phase value of the modulating low-frequency time series at time  $t$ , and  $\phi_{ut}$  to the phase value of the upper-frequency band power time series at time  $t$ . The SI is, thus, a complex number with its phase angle ( $SI_i$ ) representing the “preferred phase” of the synchronization, i.e. the phase of the lower frequency at which coupling with the upper-frequency band in terms of power modulation is maximal [50].

### Statistical analyses

For statistical analyses, we used Matlab 2019b (The MathWorks, Inc.), the open-source toolbox FieldTrip [49], the CircStat toolbox [51], SPSS (IBM SPSS Statistics, Version 24) and R (R Core Team 2020, [52]). Comparisons between groups (ASD vs TD) mostly relied on analyses of variance (ANOVA) including, besides the Group factor, a repeated measures topography factor (frontal, central, parietal) and, for spindle analyses a repeated measures spindle type factor (fast, slow). Degrees of freedom were Greenhouse–Geisser corrected. The timing of co-occurrence of spindles during SOs as visualized in peri-event time histograms was evaluated by testing against averaged bin shuffled surrogate data (5,000 permutations) from each individual using a dependent samples t-test and correcting for multiple comparisons by a cluster-based permutation test (Monte Carlo Method, 5,000 permutations, cluster  $\alpha < .05$ ) as implemented in FieldTrip [53].

SO-baseline contrasts were statistically tested against zero and a cluster-based permutation test (as described above) was used to correct for multiple comparisons. To further test power differences between ASD and TD children, we used independent samples t-tests, again correcting for multiple comparisons by applying a cluster-based permutation test. To test whether the preferred phase angles of SO–spindle synchronization within each participant were distributed nonuniformly and thus clustered toward one direction, we used the Rayleigh test (as implemented in the CircStat Toolbox [51]). On the group level, the V-test was used to test whether the preferred phases were nonuniformly distributed toward an a-priori defined direction. Our a-priori hypotheses were that fast spindle activity is maximally synchronized toward the SO-upstate peak (i.e. at  $0^\circ$ ) and slow spindle activity is maximally synchronized toward the downstate peak (i.e.  $\pm 180^\circ$ ). Group differences in preferred phase angles were evaluated using the Watson Williams test (circular equivalent to two-sample t-test). We evaluated the mean resultant vector length within and across participants. The vector length (ranging from 0 to 1) reflects how consistently the (mean) preferred phases are clustered toward a direction across SO events within a subject or across subjects and is further referred to as “coupling strength” [7, 14].

Correlation analyses were used to investigate the link between SO–spindle coupling and overnight memory performance. Because of the non-normal distribution of the target memory measures, Spearman’s correlations were calculated separately for the groups as well as across both groups. Additionally, to exclude a substantial bias by outliers, we calculated Kendall’s tau, which is considered more robust in the presence of outliers (e.g. [54]). However, these analyses essentially confirmed the Spearman coefficients, and will not be reported here. We performed circular linear correlations (as implemented in the CircStat toolbox) for correlations with the preferred phase

**Table 1.** Characteristics of slow oscillations and of slow (9–12 Hz) and fast spindles (12–15 Hz) during non-REM sleep

	TD M (SEM)			ASD M (SEM)			Group comparisons ( <i>p</i> )		
	Frontal	Central	Parietal	Frontal	Central	Parietal	Frontal	Central	Parietal
<b>Slow oscillations</b>									
Density per 30 sec epoch	3.31 (0.06)	3.11 (0.06)	2.98 (0.06)	3.26 (0.09)	3.04 (0.07)	2.93 (0.07)	.618	.524	.58
Duration (ms)	1.08 (0.01)	1.09 (0.01)	1.08 (0.01)	1.07 (0.01)	1.08 (0.01)	1.08 (0.01)	.799	.819	.74
Amplitude (μV)	294 (6.45)	267 (6.1)	224 (6.26)	282 (11.44)	266 (9.87)	221 (10.38)	.337	.914	.799
<b>Slow spindles</b>									
Density per 30 s epoch	2.19 (0.06)	1.75 (0.05)	1.57 (0.05)	2.16 (0.08)	1.79 (0.08)	1.63 (0.07)	.73	.699	.406
Duration (ms)	0.91 (0.01)	0.88 (0.01)	0.9 (0.02)	0.91 (0.02)	0.88 (0.01)	0.89 (0.02)	.924	.872	.626
Amplitude (μV)	57.27 (2.54)	41.51 (1.44)	35.3 (1.25)	58.86 (4.22)	42.37 (2.8)	35.49 (2.59)	.746	.784	.948
<b>Fast spindles</b>									
Density per 30 s epoch	2.25 (0.06)	2.34 (0.06)	2.11 (0.08)	2.29 (0.05)	2.39 (0.05)	2.18 (0.06)	.642	.536	.479
Duration (ms)	0.95 (0.01)	0.99 (0.02)	1.05 (0.02)	0.95 (0.01)	0.98 (0.02)	1.02 (0.02)	.908	.623	.161
Amplitude (μV)	40.72 (1.85)	35.6 (1.36)	28.86 (1.14)	42.05 (2.21)	35.84 (2.08)	29.11 (2.26)	.645	.921	.922

TD, typically developing; ASD, autism spectrum disorder; SEM, standard error of the mean. *p* is indicated for statistical comparisons between groups.

angles, and again Spearman's coefficients for the correlations with coupling strength and power derived from TFRs. In case analyses required the comparison of the angular and linear data, we used the transformed preferred phase, i.e. we calculated the absolute distance of SO–fast spindle coupling to the SO upstate (0°). For TFRs, correlation results were tested against a bootstrapped distribution (5,000 samples) of the same and corrected for multiple testing using cluster-based tests. These analyses were restricted to the SO upstate (200–800 ms after the SO negative peak) and the fast (12–15 Hz) spindle band considered to be most critical for memory consolidation. For group comparisons of correlation coefficients and comparison of dependent correlations, we used a percentile bootstrap method [55, 56]. First, 1,000 samples from each group were drawn (with replacement and keeping dependencies of observation pairs within each group). For each sample, Spearman correlations and differences of the correlation coefficients between each group's samples were computed. The resulting distribution was used to compute a 95% confidence interval (CI). The same was done for the overlapping case, where resampling was done from the whole sample.

## Results

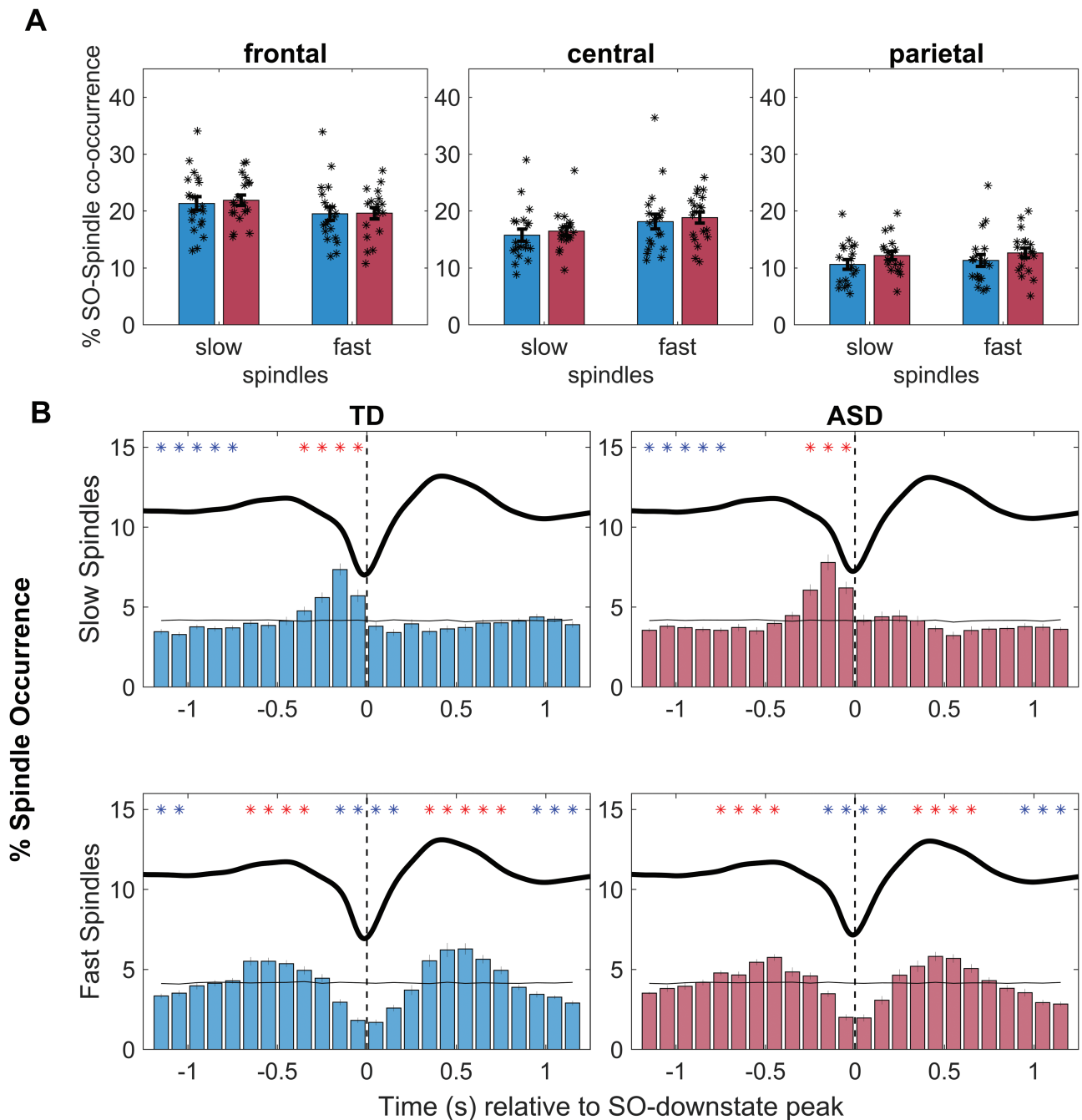
Results (including statistical comparisons) of overnight memory performance and sleep architecture for the ASD and TD children are summarized in Table S1, as reported previously [29]. Whereas overnight retention on the picture recognition task was comparable between ASD and TD children, on the DRM task, sleep in the ASD children, relative to wake performance produced an enhanced recall of critical lure words (i.e. formation of gist-based memory), compared with TD children, while recall of list words (i.e. veridical memory) was diminished in the ASD children. Sleep stage architecture (including EEG spectral power in characteristic frequency bands) was closely comparable between the groups.

Table 1 summarizes characteristics of SO and fast and slow spindle events identified during non-REM sleep in the ASD and TD children. SO amplitude and density were highest in frontal and lowest in parietal recordings ( $F(2,72) = 151, p < .001, \eta^2_p = .81$  and  $F(1.4,50) = 67, p < .001, \eta^2_p = .65$ , respectively, for Topography main effects). SO duration was longest at central

sites ( $F(1.5,55) = 5.61, p = .011, \eta^2_p = .14$ ). The amplitude of fast and slow spindles also decreased from frontal to parietal sites ( $F(1.4,50) = 130, p < .001, \eta^2_p = .78, F(1.1,41) = 204, p < .001, \eta^2_p = .85$ , respectively, for topography main effects). Generally, the amplitude was higher for slow than fast spindles, with the greatest difference in frontal channels ( $F(1.1,41) = 90, p < .001, \eta^2_p = .71$ , for Spindle type  $\times$  Topography, Table 1). Spindle density was higher for fast than slow spindles, especially in central and parietal recordings ( $F(1.4,50) = 109, p < .001, \eta^2_p = .75$ , Spindle type  $\times$  Topography). Fast spindle density was maximal at central recording sites ( $F(1.7,60) = 28, p < .001, \eta^2_p = .44$ ) whereas slow spindle density decreased from frontal to parietal derivations ( $F(1.5,52) = 186, p < .001, \eta^2_p = .84$ ). Spindle duration was generally longer for fast than slow spindles ( $F(1,36) = 165, p < .001, \eta^2_p = .82$ ), and for fast spindles shortest and for slow spindles longest at frontal sites ( $F(2,72) = 46, p < .001, \eta^2_p = .56, F(1.7,62) = 4.1, p = .028, \eta^2_p = .10$ , respectively, for topography main effects). Neither SOs (all  $p > .337$ ) nor fast or slow spindles (all  $p > .16$ ) showed any significant difference in amplitude, density or duration between ASD and TD groups.

## Slow oscillation–spindle coupling

The proportion of SOs (relative to the total number of identified SOs) co-occurring with a fast spindle ( $\pm 1.2$  s around the negative SO peak) was highest in frontal and lowest in parietal recordings ( $F(2,72) = 97, p < .001, \eta^2_p = .73$ ), and this frontal focus of co-occurrence appeared to be even more distinct for slow spindles ( $F(2,72) = 37, p < .001, \eta^2_p = .50$ , Spindle type  $\times$  Topography,  $F(2,72) = 307, p < .001, \eta^2_p = .90$ , for topography in a sub-ANOVA on slow spindles). SO–spindle co-occurrence did not differ between ASD and TD children (all  $p > .18$ ; Figure 1A). The peri-event time histograms in Figure 1B illustrate the temporal distribution of spindles co-occurring with a SO. As expected from findings in adults [12], the occurrence of fast spindles was increased during the SO upstates, i.e. in  $\sim 300$ – $700$ -ms intervals preceding and following the negative SO peak, and suppressed during the downstate, i.e.  $\pm 200$  ms around the negative SO peak (see Figure 1B for statistical significances). By contrast, the occurrence of slow spindles showed a maximum shortly before the negative SO peak. Importantly, the temporal distributions in the co-occurrence of fast or slow spindles during SO events were



**Figure 1.** Slow oscillation–spindle co-occurrence. (A) Mean (+SEM) percentages of SOs (with reference to total number of SOs) co-occurring with a slow and fast spindle, respectively, within  $\pm 1.2$  s around the negative SO-downstate peak, for typically developing (TD, blue) and autism spectrum disorder (ASD, red) children (dotplots overlaid). (B) Peri-event time histograms depicting the rate of slow (upper panel) and fast spindle occurrence (lower panel) within 100-ms bins  $\pm 1.2$  s around the SO downstate peak (0 s, vertical dashed line) at frontal cortical recording sites for TD (left) and ASD (right) children. Asterisks depict significant increases (red) and decreases (blue) in spindle occurrence compared to surrogate data (black solid line, all cluster  $p < .002$ , dependent samples t-tests, corrected for multiple comparisons using cluster-based permutation tests). Groups did not differ in their distribution of spindle occurrence.

closely comparable between ASD and TD children (all clusters for group comparisons,  $p > .08$ ).

TFRs confirmed the picture from peri-event time histograms, indicating significant increases in 12–15 Hz fast spindle power around 500 ms before and after the negative SO peak, i.e. during the SO upstates, and a single and most distinct increase in 9–12 Hz slow spindle power in the up-to-down transitions of the SO, shortly ( $\sim 100$  ms) before the negative SO peak (Figure 2). The

increase in power in the slow spindle band at the SO up-to-downstate transition clearly extended into lower frequencies, reaching a maximum at 5–7 Hz. Generally, these spindle-related power modulations were stronger at frontal and central than parietal electrode sites. There were no differences between ASD and TD children (for all clusters  $p > .17$ , independent samples t-tests, corrected for multiple comparisons using cluster-based permutation tests).

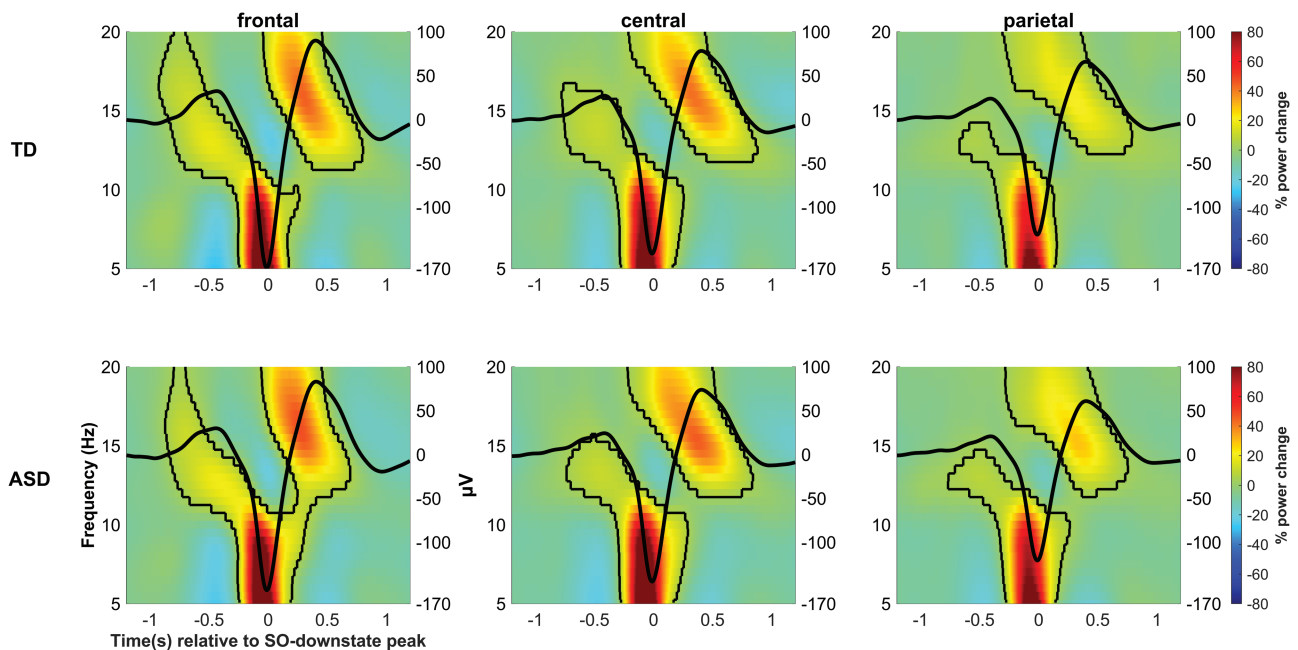


**Figure 2.** Time–frequency representations (TFR) of SO events. Spectral power in the 5–20 Hz (left y-axis) band in a  $\pm 1.2$ -s window around the SO-downstate peak (0 s) at frontal (left), central (middle), and parietal (right) recording sites, for TD (top) and ASD (bottom) children. Power is color coded (right bars) and indicated as percent change with reference to average power in a  $\pm 1.5$ -s window around the SO-downstate peak). The average SO from the respective recording site is superimposed (black line, amplitude in  $\mu\text{V}$  right y-axis). Thin black lines indicate significant positive clusters (all cluster  $p < .001$ , SO vs average power contrasts tested against zero, corrected for multiple comparisons by cluster-based permutation test). Significant negative clusters are outlined in [Figure S1](#).

To further test the phase relationship between the SO frequency band (0.5–1.25 Hz) and the two spindle frequency bands, we calculated the “preferred phase” of synchronization (see Methods). These analyses confirmed in both TD and ASD groups (and at all recording sites) that the coupling of fast spindle activity to the SO cycle was maximal shortly before the SO-upstate peak ( $0^\circ$ ; all  $p < .001$ , V-test) whereas slow spindle activity was most strongly coupled to the SO around the negative SO peak ( $\pm 180^\circ$ ; all  $p < .025$ , V-test), with no differences between ASD and TD groups (all  $p > .180$ , Watson Williams test; [Figure 3](#), preferred phase angles and group comparisons are presented in [Table S2](#)). The groups did not differ in coupling strength, i.e. how consistently preferred phases of SO–spindle coupling were clustered toward the same direction (all  $p > .476$ ). Analyses on the subject level revealed a nonuniform distribution ( $p < .05$ , Rayleigh test) of the preferred phases of fast spindle synchronization (across all individual SO events) in 18 out of 20 TD children and in 15 out of 19 ASD children. For slow spindle activity 18 out of the 20 TD, and 16 out of the 19 ASD children showed a nonuniform distribution ([Figure 3](#)).

### Correlation analyses

We correlated overnight memory performance in the children with sleep SO and spindle activity. In light of growing evidence for the importance of precise SO–spindle coupling underlying effective memory consolidation during sleep [[7–9](#), [14](#)], we focused our analysis on the “preferred phase” and “coupling strength” of SO–spindle coupling and how these measures were related to the two target memory measures: i.e. recognition memory on the picture recognition task (across neutral and negative pictures) and the recall of critical lures on the

DRM task (recalled critical lures divided by total – veridical plus critical lure – word recall), as a measure of gist memory formation. The analyses revealed no consistent correlations of memory performance with SO–slow spindle coupling (across groups: all  $r < .37$ ,  $p > .09$ ), but several distinct relationships with SO–fast spindle coupling.

Picture recognition benefitted from sleep in both ASD and TD children with no difference between groups. Importantly, the circular linear correlation between the preferred phase angle of SO–fast spindle coupling at frontal sites and recognition performance showed better recognition performance the closer the peak of fast spindle activity was to the SO-upstate peak. This correlation reached significance only in the TD children ( $r = .61$ ,  $p = .02$ , [Figure 4A](#), top). It was not significant in the ASD children ( $r = .17$ ,  $p = .77$ ) or across groups ( $r = .25$ ,  $p = .31$ ), and also the difference in coefficients between groups was not significant (CI  $[-0.18, 0.64]$ ,  $p = .24$ ). Recognition performance did not correlate with coupling strength (all  $p > .16$ , [Figure 4A](#), bottom). Correlating power in TFRs time-locked to the negative SO peak with recognition performance, revealed that higher frontal fast spindle activity during the SO upstate ( $-400$  ms after the SO negative peak) is associated with better memory retention across both groups (mean cluster  $r = .37$ , cluster  $p = .01$ ; [Figure 4B](#)). However, overall, this relationship appeared to be weak as no significant clusters were detected for correlations calculated separately for the TD and ASD groups.

Separate analyses on SO and spindles in isolation revealed a correlation of picture recognition with fast spindle density across groups that was most pronounced at central recording sites ( $r = .44$ ,  $p = .005$ ) and somewhat less at frontal sites ( $r = .29$ ,  $p = .07$ ). This association was similar in TD (central:  $r = .54$ ,  $p = .02$ ) and ASD children (central:  $r = .53$ ,  $p = .02$ ). Spindle density was moderately but consistently correlated with the preferred

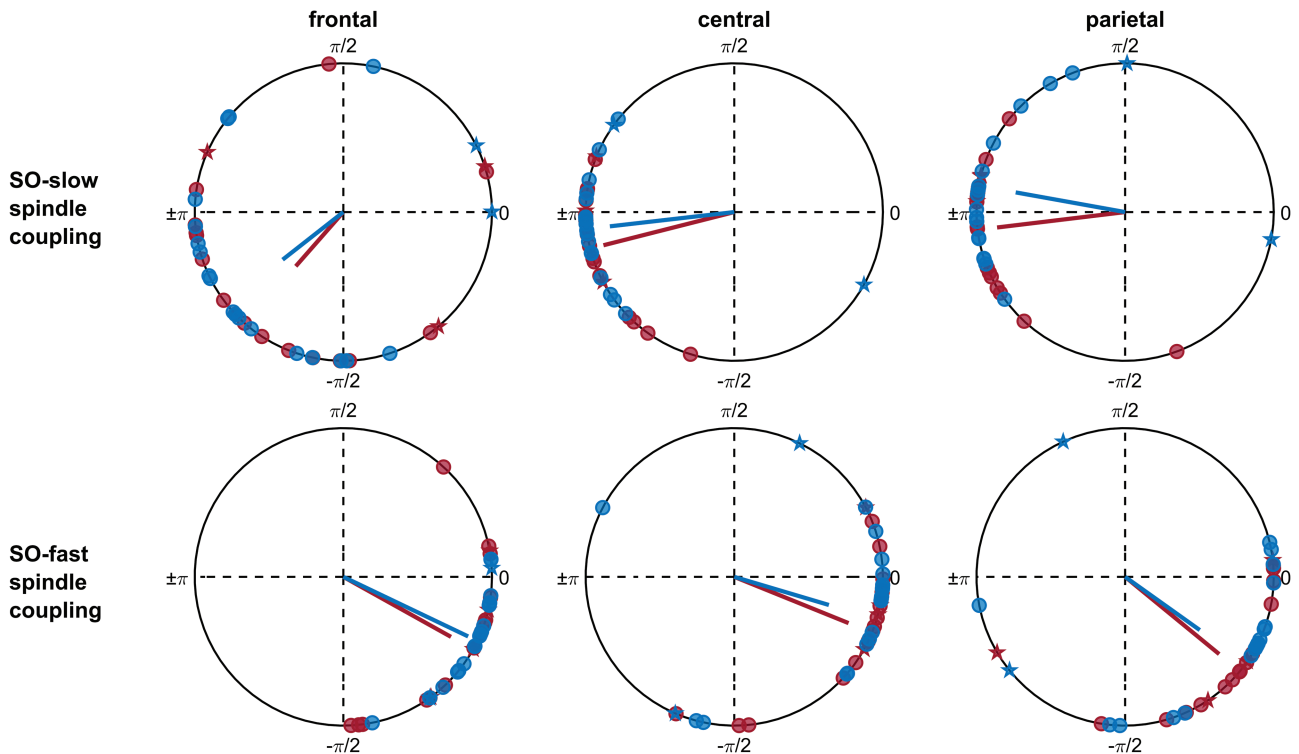


**Figure 3.** Preferred phase of SO-spindle coupling. Mean preferred phase (red and blue dots and asterisks) and coupling strength (red and blue lines) for the coupling of slow spindles (upper panels) and fast spindles (lower panels) to the SO cycle ( $0^\circ$  SO-upstate peak,  $\pm 180^\circ$  SO-downstate peak) at frontal (left), central (middle), and parietal (right) recording sites, for TD (blue) and ASD (red) children. Red and blue dots indicate the mean preferred phase of those individuals with a significant (Rayleigh test,  $p < .05$ ) nonuniform distribution of preferred phase angles of synchronization across SO event (thus clustering toward one direction). Asterisks indicate individuals with a uniform distribution. The mean resultant vector length reflects how consistently the individual mean preferred phases in a group are distributed toward the same phase angle. TD and ASD groups did not differ in their mean preferred phase of synchronization (Watson-Williams test, all  $p > .18$ ). Both groups showed maximum coupling of fast spindle activity shortly before the SO positive peak ( $0^\circ$ ; TD: on average at  $-26^\circ$ , ASD on average at  $-30^\circ$ ) and of slow spindle activity around the SO downstate peak ( $\pm 180^\circ$ ; TD: on average at  $-169^\circ$ , ASD on average at  $-157^\circ$ ). See [Table S2](#) for a summary of group comparisons

phase (absolute distance to SO-upstate peak) of SO-fast spindle coupling (across groups, frontal  $r = -.32$ ,  $p = .047$ , central  $r = -.36$ ,  $p = .026$ , parietal  $r = -.39$ ,  $p = .014$ ), leaving the possibility that spindle density contributed to mediating the effects of SO-spindle coupling. Indeed, comparison of association strength of picture recognition with either spindle density or preferred phase, suggested for the central electrode site a greater influence of spindle density than preferred phase (across groups: CI  $[-1.11, -0.25]$ ,  $p < .001$ ). For the frontal recordings, these analyses showed across groups no difference in correlation strength (CI  $[-1.02, 0.08]$ ,  $p = .088$ ), and for subanalyses in TD children a tendency for a greater influence of the preferred phase (CI  $[-1.42, 0.001]$ ,  $p = .052$ ; ASD:  $p = .596$ ).

On the DRM task, the sleep-associated gain in the recall of critical lures was greater in ASD than TD children. The preferred phase of SO-fast spindle coupling did not correlate with the recall of critical lure words across both groups (all  $r < .32$ , all  $p > .15$ ) or in separate analyses of TD and ASD groups (all  $r < .45$ , all  $p > .13$ , [Figure 5A](#) for parietal recording site). For the coupling strength, a significant correlation with critical lure recall was revealed in parietal recordings across groups which, surprisingly, was in the negative direction ( $r = -.37$ ,  $p = .02$ ). Separate analyses of both groups revealed a significant negative correlation in the children with ASD ( $r = -.64$ ,  $p = .003$ ) whereas in the TD children this correlation was not significant ( $r = -.17$ ,  $p = .49$ ), with the difference of coefficients between the groups approaching significance (CI  $[-0.96, 0.06]$ ,  $p = .07$ ). The correlation reflected

that recall of critical lures, was the higher the less consistent the phase angles of SO-fast spindle coupling was across an individual's SO events. Correspondingly, correlating critical lure recall with power in parietal TFR (time-locked to the SO negative peak) revealed a significant negative cluster for the 12–15 Hz fast spindle band 300–600 ms after the SO negative peak, indicating that enhanced critical lure recall was associated with reduced fast spindle power during the SO-upstate. This cluster reached significance in analysis across both groups (mean cluster  $r = -.39$ , cluster  $p = .025$ ), and in a separate analysis of the ASD children (mean cluster  $r = -.58$ , cluster  $p = .006$ , [Figure 5B](#)) but not TD children. To evaluate whether correlation coefficients differed, the mean power of the time-frequency bins corresponding to the significant cluster across groups were used, which did not significantly differ (CI  $[-0.84, 0.14]$ ,  $p = .14$ ).

Analyses of SOs and spindles in isolation revealed that critical lure recall was negatively associated with SO amplitude across groups and at all frontal, central and parietal recording sites ( $r < -.40$ ,  $p < .01$ ). This relation was also observed in the ASD ( $r < -.63$ ,  $p < .004$ ), but not in the TD children (all  $p > .3$ ), with the difference between the group's coefficients being significant at the frontal recording sites (CI  $[-1.13, -0.06]$ ,  $p = .03$ ). Importantly, we found that SO amplitude showed also a distinct positive association with coupling strength across groups ( $r = .61$ ,  $p < .001$ ), in ASD children ( $r = .74$ ,  $p < .001$ ) and in TD children ( $r = .49$ ,  $p = .03$ ) suggesting that SO amplitude might confound the negative association of coupling strength and critical lure recall.

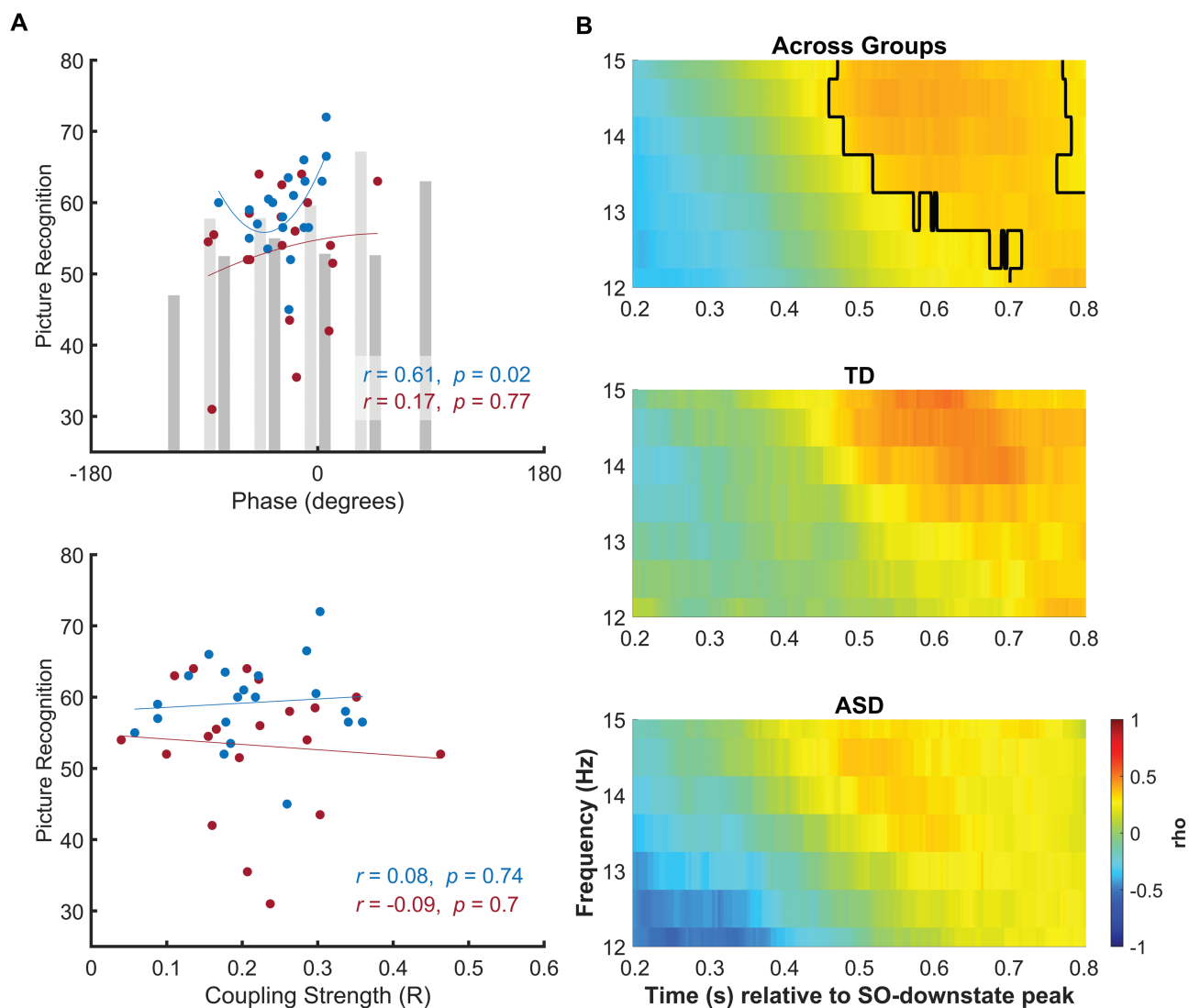


**Figure 4.** Association of SO–spindle coupling and visual recognition memory. (A) Correlation of number of recognized pictures (y-axis) with the individual mean preferred phase of SO–fast spindle coupling (top) and the individual coupling strength (bottom) at frontal recordings, for TD (blue dots and lines) and ASD (red) children. Top panel indicates circular linear correlations with the phase angle. Additional bars depict mean memory performance of participants with their preferred phase angle binned to nine overlapping bins (bin size 80°, each  $\pm 40^\circ$  overlap, TD: light gray, ASD: dark gray). Blue (TD) and red (ASD) lines depict a quadratic fit to approximate the nonlinear relation. Significant correlation in TD children indicates better recognition performance the closer the preferred phase of fast spindle activity is to the SO upstate peak. (B) Correlation (color coded, right bar) between power in TFRs (from frontal cortical recordings) and picture recognition, calculated across both groups (top), and separately for TD (middle) and ASD (bottom) children. Significant clusters are outlined (across groups: mean cluster  $r = .37, p = .01$ ).

Thus, partializing out SO amplitude nullified the association of coupling strength and critical lure recall (across groups:  $r = -.07, p = .64$ , ASD:  $r = -.27, p = .28$ , TD:  $r = -.09, p = .73$ ). In contrast with SO amplitude, fast spindle density was positively associated with critical lure recall across groups and in all channels ( $r > .37, p < .03$ ). This relationship was also evident in TD children ( $r > .68, p < .002$ ), but not in the ASD children (all  $p > .2$ ), with the difference in coefficients between groups reaching significance for parietal recording sites (CI  $[-1.19, -0.03], p = .04$ ).

## Discussion

In light of recently growing evidence that efficacy of memory processing during sleep is closely linked to the synchronization of sleep spindle activity to the SO–upstate during non-REM

sleep [7–9, 14, 57], here we aimed at a fine-grained reanalysis of the sleep EEG of a foregoing study in 9–12 years old TD children and children with ASD without intellectual impairment, to identify mechanisms underlying the sleep-associated consolidation of visual recognition memories and gist memory (for critical lures) in the DRM task [29]. That study revealed a comparable benefit from sleep for visual recognition memory in both groups, whereas the overnight abstraction of gist memory in terms of critical lure recall, was enhanced in ASD patients although, notably, the macro-architecture of sleep and sleep stages was closely comparable between the groups. Here, we found that SO–spindle coupling itself in ASD children does not differ from that in TD children. The overnight retention of visual recognition memories in the TD children was positively correlated with SO–fast spindle coupling (at frontal cortical sites). Although this relationship appeared to be not very robust in the children, the

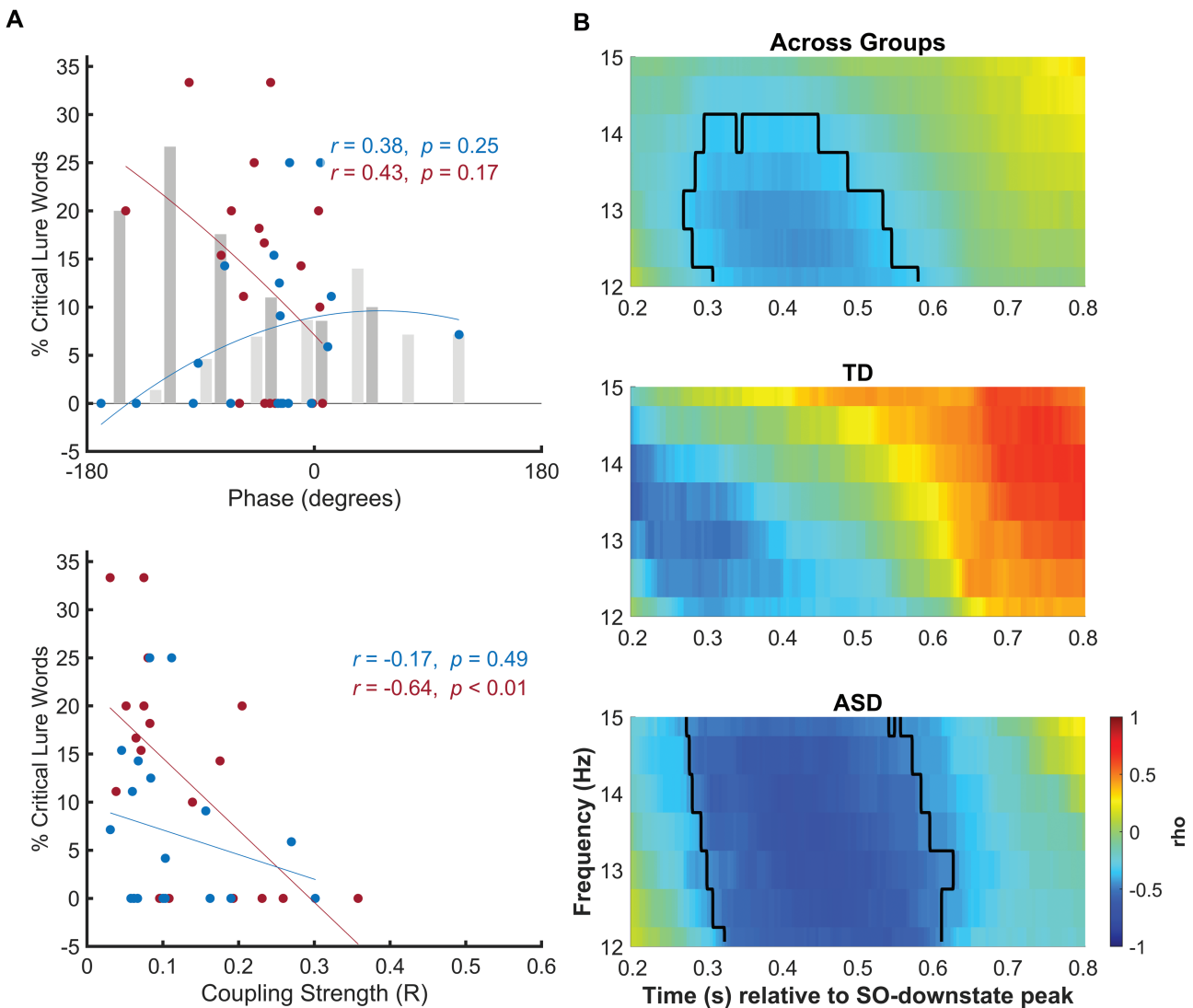


**Figure 5.** Association of SO–spindle coupling and recall of critical lure words. (A) Correlation of critical lure recall on the DRM task (in percent of total word recall, y-axis) with the individual mean preferred phase of SO–fast spindle coupling (top) and the coupling strength (bottom) at parietal recordings, for TD (blue dots and lines) and ASD (red) children. Top panel indicates circular linear correlations with the phase angle. Additional bars depict mean memory performance of participants with their preferred phase angle binned to nine overlapping bins (bin size 80°, each  $\pm 40^\circ$  overlap, TD: light gray, ASD: dark gray). Blue (TD) and red (ASD) lines depict a quadratic fit to approximate the nonlinear relation. Significant correlation of coupling strength in ASD children indicates more critical lures are recalled the less consistently fast spindle activity is coupled to the SO phase across SO events. (B) Correlation (color coded, right bar) between power in TFRs (from parietal cortical recordings) and critical lure recall, calculated across both groups (top), and separately for TD (middle) and ASD (bottom) children. Significant clusters are outlined (across groups: mean cluster  $r = -.39$ ,  $p = .025$ , ASD: mean cluster  $r = -.58$ ,  $p = .006$ , TD: no sign. clusters).

finding extends previous observations of a similar relationship in adults and children [7, 14]. In addition, picture recognition performance was consistently correlated with spindle density (at central sites) in both TD and ASD children. In stark contrast with our hypothesis, we found that overnight gist memory abstraction on the DRM task in the ASD children was negatively correlated with SO–fast spindle coupling and remained uncorrelated in the TD children. Our findings point to functional differences in memory processing during sleep in children with ASD without intellectual impairment.

Our findings extend our previous findings [29] in showing that not only the macroarchitecture of sleep stages but also the micro-architecture comprising the characteristic stage-specific oscillations are, in central aspects, closely comparable in children with ASD to that of TD children. Spindle and SO events

in our ASD children did not differ from those in TD children, in amplitude, density, duration, or topography. Moreover, both groups showed, especially over the frontal cortex, a robust modulation of spindle activity during the SO cycle such that fast spindle activity was suppressed during the SO–downstate and distinctly increased in the (subsequent) SO–upstate, whereas slow spindle activity showed a distinct increase in the up-to-down transition of the SO, shortly before the downstate peak. These findings replicate the well-established pattern of SO–spindle coupling in adults [7, 12, 13, 58] and prove a sufficient maturation of the frontal cortex and thalamic structures underlying the co-ordinate generation of SOs and spindles with no differences between our TD and ASD children [59, 60]. In fact, our study, being the first to analyze precise SO–spindle coupling in children with ASD, revealed that the SO–upstate related

increases in fast spindle power, with regard to the preferred phase angle and distribution of phase angles in this coupling, were very similar in TD and ASD children. Coupled SO-spindles have been shown to couple with hippocampal ripples (which are not accessible in healthy humans), with this triple-coupling supporting the hippocampo-neocortical redistribution and systems consolidation of hippocampus-dependent memory representations during sleep [3, 6]. Against this backdrop, our findings revealing a remarkable similarity even in the precise timing of SO-spindle coupling between TD and ASD groups, strongly suggest the underlying machinery of systems consolidation during sleep to be fully intact in this sample of children with ASD.

However, we found subtle differences between the groups in how the precise timing of SO-spindle coupling correlates with overnight memory processing, suggesting a functional difference between the groups. Overnight retention of visual recognition memories was better the closer the maximum coupling of frontal SO and spindles was to the SO-upstate peak. This correlation, which was more pronounced in the TD children, was weaker and nonsignificant in the children with ASD, although the difference between groups did not reach significance. The finding might reflect an altered functionality of frontal SO-spindle coupling for memory processing in the ASD children, a view that is further supported by the analyses of DRM performance (see below).

Results from analyses of DRM performance were surprising inasmuch, in the TD children critical lure recall was not correlated with any measure of SO-spindle coupling, but only showed a strong correlation with spindle density (assessed independently of SOs). The association with spindle activity in our TD children agrees with previous studies in adults where spindle activity was positively correlated not only with critical lure recall on the DRM task but also with measures of gist memory formation in other task paradigms [61, 62]. However, in other studies, this correlation was not observed in adults or children [63, 64]. For example, examining ~17 years old adolescents on the DRM task, Kuula et al. [65] found no correlation between spindle density and critical lure recall in boys, and in girls even a negative correlation. Assessments of SOs and SWS-related measures in general provide a likewise mixed picture [64, 66, 67]. Several studies in adults found a negative correlation between recall of critical lures and SWS time [68, 69]. Thus, in combination with these foregoing studies, our failure to find a link between critical lure recall and SO-spindle coupling in the TD children challenges the idea that such coupling plays also a key role for abstracting gist during sleep-dependent memory formation. The function of SO-fast spindle coupling, in this regard, might be restricted to facilitating hippocampo-to-neocortical transmission of reactivated memory information, whereas the abstraction of gist appears to depend on further processes that are independent of or may even competitively interact with SO-spindle-related memory processing.

This view is strongly supported by the present findings in ASD children who displayed an overall greater gain in gist abstraction from sleep than TD children, and who showed a strong correlation in negative direction between the strength of SO-spindle coupling (over parietal cortex) and recall of critical lures. In addition, recall of critical lures in the ASD children was negatively associated with SO amplitudes, i.e. critical lure recall was better the lower the SO amplitude was. Note, these correlations well discriminated ASD from TD children where the respective

coefficients remained nonsignificant. Because correlation analyses also revealed a general and strong association of high SO amplitude with high SO-spindle coupling strength, the present data do not allow to answer whether SO amplitude itself or the coupling of SO with fast spindles is the primary factor that counteracts critical lure recall. Physiologically enhanced depolarization during the SO upstate is expected to exert a stronger drive on thalamocortical spindle generation [70]. Whatever the case, the pattern observed here in children with ASD remarkably fits findings in healthy adults suggesting that SWS counters gist abstraction processes [66, 69]. The latter study reported a negative correlation between time spent in SWS and the recall of critical lures on the DRM task. Overall, the correlations observed here in children with ASD adds support to the conclusion that gist abstraction during sleep is linked to mechanisms that are incompatible with SO-spindle coupling and, perhaps, also with SWS in general [66]. However, this conclusion remains tentative inasmuch, in the present study, it is derived from the specific correlational pattern observed in the ASD children, whereas in our TD children sleep-associated gist abstraction appeared to be primarily linked to sleep spindle density during non-REM sleep, including both SWS and stage 2 sleep.

Although our results in showing an adult-like pattern of SO-spindle synchronization in TD children bolster our understanding of the mechanisms underlying sleep-dependent memory processing during the middle childhood period, a generalization to even earlier ages is certainly premature, considering the strong alteration SOs and spindles undergo during infancy and early childhood [59, 71, 72]. It should be similarly cautioned against overgeneralizing our results in children with ASD. In particular, the surprising similarity in sleep-related oscillatory activity between our TD and ASD groups might reflect that we relied on a rather small and perhaps nonrepresentative sample of children. Others found distinct changes in ASD children in the macroarchitecture of sleep (e.g. reduced sleep efficacy, prolonged sleep onset latency [25, 26, 30]) as well as for its microarchitecture (e.g. reduced spindle density or power, increased delta power [24, 25, 27]). Moreover, ASD children show high night-to-night variability of sleep quality [73], possibly also contributing to our finding of subjective, but not objective sleep differences between the groups. Variable outcomes might further be explained by the heterogeneity of the disorder itself or might also reflect methodological differences. For example, whereas the present study (like others, e.g. Fletcher et al. [24]) relied on an automated spindle detection procedure applied to sleep stage 2 and SWS, others used visual spindle detection procedures applied only to sleep stage 2 (e.g. [26, 27, 30]). Automated spindle detection probably provides more replicable results than visual detection but, results might change depending on changes in the detection criteria in the algorithm [74]. Age and gender (here we examined only boys) may be further factors accounting for the variability in the sleep findings among studies. For example, in a recent study, 13- to 30-months old children with ASD showed reduced theta and fast spindle-band power compared to TD children during a nap [75]. Moreover, ASD is marked by brain overgrowth in early childhood which later abnormally slows down [76].

Inasmuch as the enhanced gist abstraction during sleep in ASD children was a focus of our study, study limitations specifically related to this process also need to be considered. There is growing evidence from studies in healthy subjects that the

formation of abstracted gist memory as well as the enhancing effects of sleep on gist memory formation, might express itself only with considerable delay (e.g. [63, 77]). The Lutz et al. [63] study found an enhancing effect of sleep on gist abstraction in a DRM task at a test one year after the experimental sleep night but not one day after this night. From this point of view, our study is limited by the fact that we did not fully cover the time course of gist memory formation. The relevance of this point is underlined by studies revealing altered memory processing in ASD only in delayed test conditions [24, 78]. Thus, Fletcher and coworkers [24] found that overnight consolidation of newly learned animals was comparable in children with ASD and TD children at a test after the experimental night but, at 1-month follow up test, the ASD children recalled less details than the TD children. Although those findings of diminished memory for details fit the concept of an increased sleep-dependent abstraction of gist memory, as derived from the present results, their slow time course of emergence calls for further studies into the specific temporal dynamics of gist memory formation in ASD children.

In conclusion, our analyses identify an adult-like pattern of fast spindle activity synchronizing to the upstate of SOs which was highly comparable in our 9–12 years old TD and ASD boys without intellectual impairment. Like in adults, this SO–fast spindle coupling was positively correlated with overnight retention of visual recognition memories in the TD children, and to a less degree in the ASD children. On the other side, the sleep-dependent abstraction of gist memory on the DRM task, which was stronger in ASD than TD children, was linked to a strong negative correlation between SO–fast spindle coupling and critical lure recall in the ASD children, suggesting that gist abstraction during sleep involves different mechanisms that possibly compete with SO–fast spindle coupling and are particularly activated in children with ASD.

## Funding

This study was supported by the fortune program of the Faculty of Medicine of the University Hospital of Tübingen and by a grant from the European Research Council (ERC AdG 883098 SleepBalance) to JB.

## Acknowledgments

The authors thank Damaris Schenk and Lisa Hepp for their help in data collection, as well as all families for their participation.

## Disclosure Statement

Financial Disclosure: none.

Non-financial Disclosure: none.

## References

1. Diekelmann S, et al. The memory function of sleep. *Nat Rev Neurosci.* 2010;11(2):114–126.
2. Rasch B, et al. About sleep's role in memory. *Physiol Rev.* 2013;93(2):681–766.
3. Klinzing JG, et al. Mechanisms of systems memory consolidation during sleep. *Nat Neurosci.* 2019;22(10):1598–1610.
4. Lewis PA, et al. Overlapping memory replay during sleep builds cognitive schemata. *Trends Cogn Sci.* 2011;15(8):343–351.
5. Sekeres MJ, et al. The hippocampus and related neocortical structures in memory transformation. *Neurosci Lett.* 2018;680:39–53.
6. Latchoumane CV, et al. Thalamic spindles promote memory formation during sleep through triple phase-locking of cortical, thalamic, and hippocampal rhythms. *Neuron.* 2017;95(2):424–435.e6.
7. Helfrich RF, et al. Old brains come uncoupled in sleep: slow wave-spindle synchrony, brain atrophy, and forgetting. *Neuron.* 2018;97(1):221–230.e4.
8. Muehlroth BE, et al. Precise slow oscillation-spindle coupling promotes memory consolidation in younger and older adults. *Sci Rep.* 2019;9(1):1940.
9. Niknazar M, et al. Coupling of thalamocortical sleep oscillations are important for memory consolidation in humans. *PLoS One.* 2015;10(12):e0144720.
10. Ladenbauer J, et al. Promoting sleep oscillations and their functional coupling by transcranial stimulation enhances memory consolidation in mild cognitive impairment. *J Neurosci.* 2017;37(30):7111–7124.
11. Cox R, et al. Local sleep spindle modulations in relation to specific memory cues. *Neuroimage.* 2014;99:103–110.
12. Mölle M, et al. Fast and slow spindles during the sleep slow oscillation: disparate coalescence and engagement in memory processing. *Sleep.* 2011;34(10):1411–1421.
13. Staresina BP, et al. Hierarchical nesting of slow oscillations, spindles and ripples in the human hippocampus during sleep. *Nat Neurosci.* 2015;18(11):1679–1686.
14. Hahn M, et al. Slow oscillation-spindle coupling predicts enhanced memory formation from childhood to adolescence. *Elife.* 2020;9:e53730.
15. Piantoni G, et al. Modulation of  $\gamma$  and spindle-range power by slow oscillations in scalp sleep EEG of children. *Int J Psychophysiol.* 2013;89(2):252–258.
16. Hahn M, et al. Developmental changes of sleep spindles and their impact on sleep-dependent memory consolidation and general cognitive abilities: a longitudinal approach. *Dev Sci.* 2019;22(1):e12706.
17. Hoedlmoser K, et al. Slow sleep spindle activity, declarative memory, and general cognitive abilities in children. *Sleep.* 2014;37(9):1501–1512.
18. Wilhelm I, et al. Sleep-dependent memory consolidation—what can be learnt from children? *Neurosci Biobehav Rev.* 2012;36(7):1718–1728.
19. Prehn-Kristensen A, et al. Reduced sleep-associated consolidation of declarative memory in attention-deficit/hyperactivity disorder. *Sleep Med.* 2011;12(7):672–679.
20. Singh K, et al. Sleep in autism spectrum disorder and attention deficit hyperactivity disorder. *Semin Pediatr Neurol.* 2015;22(2):113–125.
21. Boucher J, et al. Memory in autistic spectrum disorder. *Psychol Bull.* 2012;138(3):458–496.
22. Desautunay P, et al. Memory in autism spectrum disorder: a meta-analysis of experimental studies. *Psychol Bull.* 2020;146(5):377–410.
23. Gorgoni M, et al. Sleep EEG oscillations in neurodevelopmental disorders without intellectual disabilities. *Sleep Med Rev.* 2020;49:101224.
24. Fletcher FE, et al. Atypicalities in sleep and semantic consolidation in autism. *Dev Sci.* 2020;23(3):e12906.
25. Lázár AS, et al. Reduced fronto-cortical brain connectivity during NREM sleep in Asperger syndrome: an EEG

- spectral and phase coherence study. *Clin Neurophysiol.* 2010;**121**(11):1844–1854.
26. Lambert A, et al. Poor sleep affects daytime functioning in typically developing and autistic children not complaining of sleep problems: a questionnaire-based and polysomnographic study. *Res Autism Spectrum Disord.* 2016;**23**:94–106.
  27. Tessier S, et al. Intelligence measures and stage 2 sleep in typically-developing and autistic children. *Int J Psychophysiol.* 2015;**97**(1):58–65.
  28. Tessier S, et al. REM sleep and emotional face memory in typically-developing children and children with autism. *Biol Psychol.* 2015;**110**(Suppl C):107–114.
  29. Kurz EM, et al. Signs of enhanced formation of gist memory in children with autism spectrum disorder - a study of memory functions of sleep. *J Child Psychol Psychiatry.* 2019;**60**(8):907–916.
  30. Maski K, et al. Sleep dependent memory consolidation in children with autism spectrum disorder. *Sleep.* 2015;**38**(12):1955–1963.
  31. Deese J. On the prediction of occurrence of particular verbal intrusions in immediate recall. *J Exp Psychol.* 1959;**58**(1):17–22.
  32. Roediger HL, et al. Creating false memories: remembering words not presented in lists. *J Exp Psychol.* 1995;**21**(4):803.
  33. Lerner I, et al. Sleep and the extraction of hidden regularities: a systematic review and the importance of temporal rules. *Sleep Med Rev.* 2019;**47**:39–50.
  34. Weiß RH. *Grundintelligenztest Skala 2, CFT 20-R [Basic Intelligence Test, Scale 2, CFT 20 (revised)]*. Göttingen: Hogrefe; 2006.
  35. Poustka L, et al. *ADOS-2: Diagnostische Beobachtungsskala für Autistische Störungen-2. Deutschsprachige Fassung der Autism Diagnostic Observation Schedule - 2 von C. Lord, M. Rutter, P.C. DiLavore, S. Risi, K. Gotham und S.L. Bishop (Module 1-4) und C. Lord, R.J. Luyster, K. Gotham und W. Guthrie (Kleinkind-Modul)*. Bern: Huber; 2015.
  36. Bölte S, et al. *ADI-R Diagnostisches Interview für Autismus-Revidiert. Deutsche Fassung des Autism Diagnostic Interview-Revised (ADI-R) von Michael Rutter, Ann LeCouteur und Catherine Lord*. Bern: Huber; 2006.
  37. Achenbach TM. *Manual for the Child Behavior Checklist/4–18 and 1991 Profile*. Burlington: Department of Psychiatry, University of Vermont; 1991.
  38. Bölte S, et al. *Skala zur Erfassung sozialer Reaktivität (SRS)*. Bern: Huber; 2008.
  39. Döpfner M, et al. *Diagnostik-System für psychische Störungen nach ICD-10 und DSM-IV für Kinder und Jugendliche (DISYPS-II) [Diagnostic systems for mental disorders based on ICD-10 and DSM-IV for children and adolescents]*. Bern: Huber; 2008.
  40. Stiensmeier-Pelster J, et al. *Depressions-Inventar für Kinder und Jugendliche (DIKJ)*. Göttingen: Hogrefe; 2000.
  41. Bruni O, et al. The Sleep Disturbance Scale for Children (SDSC). Construction and validation of an instrument to evaluate sleep disturbances in childhood and adolescence. *J Sleep Res.* 1996;**5**(4):251–261.
  42. Delmo C, et al. *Diagnostisches Interview Kiddie-SADS-Present and Lifetime Version 5. Aufl. der deutschen Forschungsversion*. Frankfurt am Main: Klinik für Psychiatrie und Psychotherapie des Kindes- und Jugendalters der Universität Frankfurt; 2000.
  43. Bolinger E, et al. Sleep divergently affects cognitive and automatic emotional response in children. *Neuropsychologia.* 2018;**117**:84–91.
  44. Prehn-Kristensen A, et al. Sleep in children enhances preferentially emotional declarative but not procedural memories. *J Exp Child Psychol.* 2009;**104**(1):132–139.
  45. Rechtschaffen A, et al. *A Manual of Standardized Terminology, Techniques, and Scoring Systems for Sleep Stages of Human Subjects*. Bethesda, MD: United States Department of Health, Education and Welfare; 1968.
  46. Spanò G, et al. Sleeping with hippocampal damage. *Curr Biol.* 2020;**30**(3):523–529.e3.
  47. Zinke K, et al. Children's initial sleep-associated changes in motor skill are unrelated to long-term skill levels. *Dev Sci.* 2017;**20**(6):e12463.
  48. Mölle M, et al. Slow oscillations orchestrating fast oscillations and memory consolidation. *Prog Brain Res.* 2011;**193**:93–110.
  49. Oostenveld R, et al. FieldTrip: open source software for advanced analysis of MEG, EEG, and invasive electrophysiological data. *Comput Intell Neurosci.* 2011;**2011**:156869.
  50. Cohen MX. Assessing transient cross-frequency coupling in EEG data. *J Neurosci Methods.* 2008;**168**(2):494–499.
  51. Berens P. CircStat: a MATLAB toolbox for circular statistics. *J Stat Softw.* 2009;**31**(10):21.
  52. R Core Team. *R: A Language and Environment for Statistical Computing*. Vienna, Austria: R Foundation for Statistical Computing; 2020.
  53. Maris E, et al. Nonparametric statistical testing of EEG- and MEG-data. *J Neurosci Methods.* 2007;**164**(1):177–190.
  54. Croux C, et al. Influence functions of the Spearman and Kendall correlation measures. *Stat Method Appl-Ger.* 2010;**19**(4):497–515.
  55. Wilcox RR, et al. A guide to robust statistical methods in neuroscience. *Curr Protoc Neurosci.* 2018;**82**:8.42.1–8.42.30.
  56. Wilcox RR. Comparing dependent robust correlations. *Br J Math Stat Psychol.* 2016;**69**(3):215–224.
  57. Mikutta C, et al. Phase-amplitude coupling of sleep slow oscillatory and spindle activity correlates with overnight memory consolidation. *J Sleep Res.* 2019;**28**(6):e12835.
  58. Klinzing JG, et al. Spindle activity phase-locked to sleep slow oscillations. *Neuroimage.* 2016;**134**:607–616.
  59. Kurth S, et al. Mapping of cortical activity in the first two decades of life: a high-density sleep electroencephalogram study. *J Neurosci.* 2010;**30**(40):13211–13219.
  60. Lehoux T, et al. NREM sleep EEG slow waves in autistic and typically developing children: morphological characteristics and scalp distribution. *J Sleep Res.* 2019;**28**(4):e12775.
  61. Yordanova J, et al. Sleep spindles in the right hemisphere support awareness of regularities and reflect pre-sleep activations. *Sleep.* 2017;**40**(11): doi:10.1093/sleep/zsx151
  62. Shaw JJ, et al. Lateralised sleep spindles relate to false memory generation. *Neuropsychologia.* 2017;**107**:60–67.
  63. Lutz ND, et al. Sleep supports the slow abstraction of gist from visual perceptual memories. *Sci Rep.* 2017;**7**:42950.
  64. Wilhelm I, et al. The sleeping child outplays the adult's capacity to convert implicit into explicit knowledge. *Nat Neurosci.* 2013;**16**(4):391–393.
  65. Kuula L, et al. Higher sleep spindle activity is associated with fewer false memories in adolescent girls. *Neurobiol Learn Mem.* 2019;**157**:96–105.
  66. Payne JD, et al. The role of sleep in false memory formation. *Neurobiol Learn Mem.* 2009;**92**(3):327–334.
  67. Verleger R, et al. Insights into sleep's role for insight: studies with the number reduction task. *Adv Cogn Psychol.* 2013;**9**(4):160–172.

68. Lo JC, et al. Sleep reduces false memory in healthy older adults. *Sleep*. 2014;**37**(4):665–671, 671A.
69. Pardilla-Delgado E, et al. The impact of sleep on true and false memory across long delays. *Neurobiol Learn Mem*. 2017;**137**:123–133.
70. Steriade M. Grouping of brain rhythms in corticothalamic systems. *Neuroscience*. 2006;**137**(4):1087–1106.
71. D'Atri A, et al. Different maturational changes of fast and slow sleep spindles in the first four years of life. *Sleep Med*. 2018;**42**:73–82.
72. Scholle S, et al. Sleep spindle evolution from infancy to adolescence. *Clin Neurophysiol*. 2007;**118**(7):1525–1531.
73. Fletcher FE, et al. The developmental trajectory of parent-report and objective sleep profiles in autism spectrum disorder: associations with anxiety and bedtime routines. *Autism*. 2017;**21**(4):493–503.
74. Ujma PP, et al. A comparison of two sleep spindle detection methods based on all night averages: individually adjusted vs. fixed frequencies. *Front Hum Neurosci*. 2015;**9**(52):52.
75. Page J, et al. Nonrapid eye movement sleep and risk for autism spectrum disorder in early development: A topographical electroencephalogram pilot study. *Brain Behav*. 2020;**10**(3):e01557.
76. Courchesne E, et al. Brain growth across the life span in autism: age-specific changes in anatomical pathology. *Brain Res*. 2011;**1380**:138–145.
77. Dandolo LC, et al. Time-dependent memory transformation along the hippocampal anterior-posterior axis. *Nat Commun*. 2018;**9**(1):1205.
78. Norbury CF, et al. Sound before meaning: word learning in autistic disorders. *Neuropsychologia*. 2010;**48**(14):4012–4019.